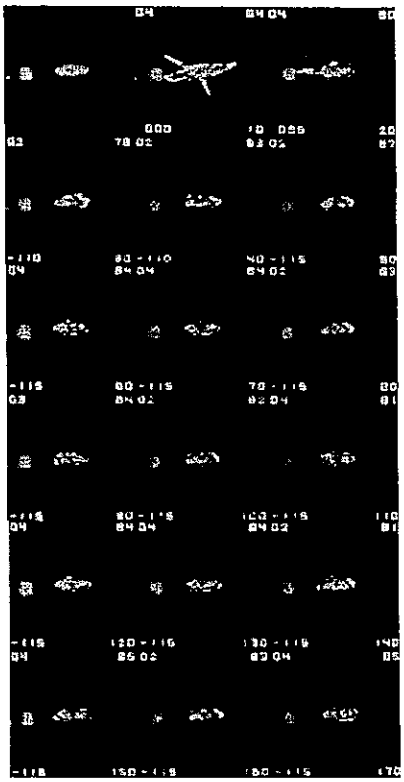

Fig. 10. Results using LL and HL in which the object is not in the model database.

TABLE I
ALGORITHM PARAMETERS

Constant	Definition	Value
W_1	low-level weight function	1.0
r^{ext}	upper bound on radii	42
M	edge filter half length	5
α_1	smoothnesss operator constant	0.4
α_2	edge operator constant	1.0
α_3	W_2 coefficient	0.1
thr_{conv}	matching convergence threshold	90%
$MAXGRAY$	maximum grey-level value	255
n	dimension of 1DCMRF (number of radii)	32

ACKNOWLEDGMENT

The authors would like to thank B. Kamgar-Parsi for his helpful comments and suggestions.

REFERENCES

[1] M. Kass, A. Witkin, and D. Terzopoulos, "Snakes: Active contour models," *Int. J. Comput. Vision*, vol. 1, pp. 321–331, 1988.

[2] P. Fua and A. J. Hanson, "Objective functions for feature discrimination: Theory," in *Proc. DARPA Image Understanding Workshop*, 1989, pp. 443–460.

[3] ——, "Objective functions for feature discrimination: Applications to semiautomated and automated feature extraction," in *Proc. DARPA Image Understanding Workshop*, 1989, pp. 676–694.

[4] R. G. Gallager, *Information Theory and Reliable Communication*. New York: Wiley, 1972, p. 80.

[5] A. Rosenfeld and A. C. Kak, *Digital Picture Processing*. New York: Academic, 1982, p. 270, vol. 2.

[6] N. Friedland and D. Adam, "Automatic cavity boundary detection from sequential ultrasound images using simulated annealing," *IEEE Trans. Med. Imaging*, vol. 8, pp. 344–353, 1989.

[7] S. Geman and D. Geman, "Stochastic relaxation, Gibbs distribution, and the Bayesian restoration of images," *IEEE Trans. Patt. Anal. Machine Intell.*, vol. PAMI-6, pp. 721–741, 1984.

[8] N. Metropolis, A. W. Rosenbluth, M. N. Rosenbluth, A. H. Teller, and E. Teller, "Equation of state calculations by fast computing machines," *J. Chem. Phys.*, vol. 21, pp. 1087–1091, 1953.

[9] S. Kirkpatrick, C. D. Gelatt Jr., and M. P. Vecchi, "Optimization by simulated annealing," IBM Res. Rep. RC 9355, 1982.

[10] E. Ising, *Zeitschrift Physik*, vol. 31, p. 253, 1925; see, for example, C. J. Thompson, *Mathematical Statistical Mechanics*. New York: Macmillan, 1972.

[11] E. B. Baum, "Graph orthogonalization," to be published in *Discrete Mathematics*.

[12] A. Margalit, "A parallel algorithm to generate a Markov random field image on a SIMD hypercube machine," CS-TR-2050, Cent. Automat. Res., Univ. of Maryland, College Park, 1988.

[13] G. H. Kornfeld, "Digital simulation of precise sensor degradation including nonlinearities and shift variance," in *Proc. SPIE Infrared Image Processing Enhancement*, vol. 781, pp. 63–70, 1987.

On Achievable Accuracy in Edge Localization

Ramakrishna Kakarala and Alfred O. Hero

Abstract—**Edge localization occurs when an edge detector determines the location of an edge in an image. In this note, we use statistical parameter estimation techniques to derive bounds on achievable accuracy in edge localization. These bounds, known as the Cramer-Rao bounds, reveal the effect on localization of factors such as signal-to-noise ratio (SNR), extent of edge observed, scale of smoothing filter, and *a priori* uncertainty about edge intensity. By using continuous values for both image coordinates and intensity, we focus on the effect of these factors prior to sampling and quantization.**

We analyze the Canny algorithm and show that for high SNR, its mean squared error is only a factor of two higher than the lower limit established by the Cramer-Rao bound. Although this is very good, we show that for high SNR, the maximum-likelihood estimator, which is also derived here, virtually achieves the lower bound.

Index Terms—**Cramer-Rao lower bound, edge detection, edge localization, maximum-likelihood estimator, mean squared error.**

Manuscript received May 23, 1990; revised August 5, 1991.

R. Kakarala is with the Department of Mathematics, University of California, Irvine, CA 92717.

A. O. Hero is with the Department of Electrical Engineering and Computer Science, University of Michigan, Ann Arbor, MI 48019-2122.

IEEE Log Number 9107545.

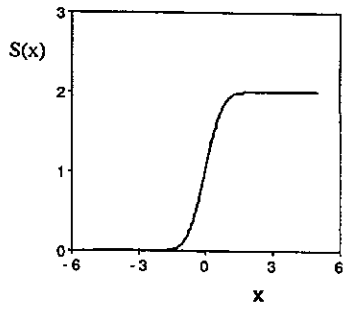

Fig. 1. Typical edge profile: A plot of $S(x;\Theta) = I\Phi(\frac{x-\ell}{\sigma_s})$ along the $x$axis with $I = 2$, $\ell = 0$, and $\sigma_s = 0.6$.

I. Introduction

For machine vision applications in mensuration [1], cartography [2], and range finding [3], the ability of edge detection algorithms to accurately determine locations of edges is crucial. These applications are more successful, in fact, if edges can be located to values *in between* pixel boundaries because this allows great accuracy with existing equipment. Algorithms that provide such "subpixel" localization capability have recently become available; we now review some examples briefly.

Tabatabai and Mitchell [4] propose a method that estimates subpixel edge locations by fitting ideal step edges, with estimated grey level moments, to image data. Huertas and Medioni [5] propose to filter the image with the Marr-Hildreth [6] $\nabla^2 G$ operator and then to use a parametric polynomial model to estimate subpixel edge locations. Hyde and Davis [7] form least-squares estimates of subpixel edge locations based only on pixel locations—and not intensities—of edge pixels, on the assumption that locations are more reliable if noise is present.

In this correspondence, we derive fundamental limits on localization accuracy that are imposed by the following factors: signal-to-noise ratio (SNR), extent of edge observed, scale of smoothing filter, and *a priori* uncertainty about edge intensity. Our analysis measures the effect of these factors prior to sampling and quantization by using continuous values for both coordinates and intensity. In particular, we focus on the minimum achievable mean squared error (MSE) in estimating an edge's location. To do so, we derive the Cramer-Rao lower bound (CRLB) on the MSE, which applies to all edge detectors with known "bias." The lower bound is then used to gauge the degree to which the popular Canny algorithm approaches the best achievable edge localization accuracy. The results of our analysis provide a theoretical basis for explaining several intuitive observations about localization that have previously appeared in the literature.

Specifically, we analyze localization error for the class of continuous edges that can be described by a 2-D blurred step edge obtained by convolving a unit step with a gaussian filter. Although our analysis allows for any orientation, for convenience, we choose x and y to be coordinate axes aligned so that the x axis goes perpendicularly across the step, and the y axis goes parallel to the step. We define the cross section in the x direction, for any fixed y, to be $\Phi\frac{x-\ell}{\sigma_s}$), where I is the intensity of the edge, ℓ is the location of the edge, σ_s is the amount of blur, and Φ is the step response of a Gaussian filter:

$$\Phi(x) = \frac{1}{\sqrt{2\pi}} \int_{-\infty}^{x} e^{-\frac{z^2}{2}} dz.$$

A typical edge profile is shown in Fig. 1.

We choose the Gaussian step edge profile for several reasons. First, step edges are the most commonly encountered edges [8]. Other kinds of profiles, such as roofs or pulses, are either far less common or can be made from linear combinations of step edges. Second, in many cases, the blurring caused by an imaging system's optics is described reasonably well by Gaussian filtering. The parameter σ_s represents, quantitatively, the amount of blur; a typical value is $\sigma_s = 0.6$ pixels [10]. Third, we do not restrict the extent of the edge in either the x or y directions; this allows us to study the effects of various observation windows without fixing arbitrary cutoffs. Other researchers have proposed similar models, such as the tanh profile [10], thus making our results comparable.

We model the received edge $r(x,y)$ to be the edge described above corrupted by additive white gaussian noise (AWGN), i.e., $r(x,y) = I\Phi(\frac{x-\ell}{\sigma_s}) + n(x,y)$, where $n(x,y)$ is a sample of AWGN. We do not claim that AWGN is physically realized in imaging systems, but rather, we use AWGN because it is a tractable model that does not assume any local structure to the noise. The AWGN model has also been used by many other researchers [1], [8], [10], which makes our results comparable. We define N_0^2 to be the variance of the AWGN process, i.e., $E[n^2(x,y)] = N_0^2$. Finally, we define SNR to be the ratio $\frac{I^2}{N_0^2}$ of the square of edge amplitude to the variance of noise.

Other researchers have studied localization performance, and we now summarize their contributions. Berzins [11] studies errors caused by corners, curves, and nonlinear illumination on laplacian-based edge operators but does not consider effects of quantization or noise. Havelock [12] considers quantization effects on localization error but does not consider noise-induced errors. Gonsalves [13] uses the Cramer-Rao approach to determine limits on accuracy in estimating the width of a 1-D pulse. These results proved useful for Burnett and Huang [2], who use them to evaluate their algorithm's performance in mensuration tasks.

We take a Cramer-Rao approach similar to Gonsalves, but for the problem of estimating the *location* of a 2-D step edge. What distinguishes our results from previous work is that we use the CRLB to answer the following questions about edge localization:

1. What is the impact on achievable MSE due to varying SNR, extent of edge observed, and *a priori* uncertainty about intensity?
2. How close to optimal are the Canny [8] and the maximum-likelihood (ML) edge localization algorithms in the sense of achieving the CRLB?

We consider the first question in Section II. In Section III, we show that for high SNR, the MSE of the Canny algorithm is only a factor of two higher than the CRLB. Finally, in Section IV, we show that for high SNR, the ML estimate of edge location actually achieves the CRLB.

In what follows, we omit details of our calculations. These can be found elsewhere [14].

II. The CRLB

Our edge profile $I\Phi(\frac{x-\ell}{\sigma_s})$ has three parameters: I, ℓ, and σ_s. In what follows, we assume that σ_s, which is the amount of blur imposed by the lens, has been measured and is thus known *a priori*. We combine the remaining unknown parameters into a vector $\Theta = [\theta_1, \theta_2] \stackrel{\text{def}}{=} [\ell, I]^T$, where the superscript T denotes transpose, and define $s(x,y;\Theta) = I\Phi(\frac{x-\ell}{\sigma_s})$. Then ℓ is the inflection point of any x cross section as $\frac{\partial^2}{\partial x^2} s(x,y;\Theta) = 0$ when $x = \ell$. In our analysis, we treat ℓ and I as "nonrandom" variables [17], which means simply that they are unknown quantities about which we do not have sufficient information to give probability distributions.

For the observed blurred and noise-corrupted edge $r(x,y) = s(x,y;\Theta) + n(x,y)$, let $\hat{\ell}(r)$ be any estimator of the edge location ℓ. Although edge detectors that give position estimates [6], [8], [10]

give both x and y coordinates to the edges that they mark, in what follows, we use only the x component at some fixed y position, and we interpret this component as an estimate of ℓ. This makes sense as we have defined the x and y coordinate axes in such a way that the intensity transition occurs only in the x direction.

We now derive the Cramer-Rao bound. Let $m = m(\Theta) = E[\hat{\ell}(r)]$ be the mean function for an estimator $\hat{\ell}$, given that the true values of the unknown parameters are $\Theta = [\ell, I]^T$. Define the (row) gradient $\nabla m = [\frac{\partial m}{\partial \theta_1}, \frac{\partial m}{\partial \theta_2}]$ and $\nabla^T m$ its transpose. Then, the Cramer-Rao bound on MSE of $\hat{\ell}$ is [17]

$$E[(\hat{\ell}(r) - \ell)^2] \geq \nabla m J^{-1} \nabla^T m + (m - \ell)^2 \tag{1}$$

where J^{-1} is the inverse of the 2×2 Fisher information matrix J. The elements J_{ij} of J are [17]

$$J_{ij} = \frac{1}{N_0^2} \int\int_A \left[\frac{\partial s(x, y; \Theta)}{\partial \theta_i}\right]\left[\frac{\partial s(x, y; \Theta)}{\partial \theta_j}\right] dx dy \tag{2}$$

where $A = [-T_y, Ty] \times [-T_x, T_x]$ is the region of the image that is searched by the edge detector known as the *observation window* in the sequel.

The quantity $B(\hat{\ell}(r)) = E[\hat{\ell}(r) - \ell] = m(\Theta) - \ell$ is called the "bias" of the estimator $\hat{\ell}$ [17]. In the following, we focus on the class of estimators that are unbiased, i.e., those estimators for which $B(\hat{\ell}(r)) = 0$. There are several reasons why this class is particularly interesting. First, as we show in the Appendix, for high SNR, any linear filter-based algorithm that has zero systematic bias, such as the Canny [8] or the Marr-Hildreth [6], is approximately unbiased. By "systematic bias," we mean the error $\hat{\ell}(r) - \ell$ when there is no noise in the input, i.e., when $r(x, y) = I\Phi(\frac{x-\ell}{\sigma_s})$. In particular, Nalwa and Binford [10] show that for estimators that use either the maxima of the first derivative [8] or the zero crossings of the second derivative [6], the systematic bias is zero for our edge profile $I\Phi(\frac{x-\ell}{\sigma_s})$ (see their Appendix I with $k_1 = k_2 = 0$). Second, the ML estimator that we derive in Section IV has zero systematic bias, and since it is based on a linear filter, it also is approximately unbiased for high SNR. Third, for some algorithms, known systematic biases can be removed by using a stored look-up table [1]. In this case, the edge detector after correction is actually unbiased.

For unbiased estimators, we have $B(\hat{\ell}(r)) = 0$, or equivalently, $E[\hat{\ell}(r)] = \ell$. Then $\nabla_\Theta[m] = [1.0]$ and (1) becomes

$$E[(\hat{\ell}(r) - \ell)^2] \geq [J^{-1}]_{11} = \frac{1}{J_{11}} \frac{1}{\left[1 - \frac{J_{21}^2}{J_{11}J_{22}}\right]} \tag{3}$$

where the right-hand side is the first diagonal element of J^{-1}. By inspecting (2) and applying the Schwarz inequality, the strict bounds $0 < \frac{J_{21}^2}{J_{11}J_{22}} < 1.0$ are easily seen. Thus, we always have

$$E[(\hat{\ell}(r) - \ell)^2] \geq \frac{1}{J_{11}}. \tag{4}$$

We now derive a particularly simple form of this equation and subsequently show that for $T_x \gg \sigma_s$, the fraction $\frac{J_{21}^2}{J_{11}J_{22}} \approx 0$.

To evaluate J_{11}, we insert $s(x, y; \Theta) = I\Phi(\frac{x-\ell}{\sigma_s})$ into (2), and after simplifying, we obtain

$$E[(\hat{\ell}(r) - \ell)^2] \geq \frac{1}{J_{11}} = \frac{N_0^2\sqrt{\pi}\sigma_s}{I^2 T_y} \frac{1}{\left[\Phi(\sqrt{2}\frac{T_x - \ell}{\sigma_s}) - \Phi(-\sqrt{2}\frac{T_x + \ell}{\sigma_s})\right]}. \tag{5}$$

Notice that the term in [..] on the right is at most 1.0 and, in fact, is nearly 1.0 if $T_x \gg \sigma_s$. For *any* T_x, we have

$$E[(\hat{\ell}(r) - \ell)^2] \geq \frac{N_0^2\sqrt{\pi}\sigma_s}{I^2 T_y}. \tag{6}$$

The quantity on the right of (6) is a lower bound on the minimum achievable MSE for any unbiased estimator of ℓ. It is shown to be nearly achievable in Section IV. This provides a simple and direct relationship between achievable MSE, SNR $\frac{I^2}{N_0^2}$, blur constant σ_s, and window lengths T_x and T_y. Since the right-hand side of (6), which is independent of T_x, is always less than the right side of (5), which includes T_x, we see that increasing T_x beyond a certain point does not improve achievable MSE. In contrast, increasing T_y always improves achievable MSE. In this sense, extending the observation window to obtain additional information *across* the edge—as measured by T_x—is of limited value in improving localization accuracy, whereas extending the window to obtain additional information *along* the edge—as measured by T_y—significantly improves localization. Thus, to maximize edge localization accuracy for fixed total window area, a rotationally symmetric edge detection operator, for which $T_x = T_y$, should not be used. Rather, one should implement an operator for which $T_y \gg T_x$. Indeed, the minimum T_x required to perform accurate edge localization can be quite small. For example, $\sigma_s = 0.6$ pixels for typical images [10], and thus, $T_x = 3$ pixels makes (5) approximately equal to its limiting form (6). Canny [8] observed this same asymmetry between T_x and T_y by using a different argument and thus chose elongated edge-oriented filters as opposed to rotationally symmetric operators for his algorithm.

We can also show, on substituting for $s(x, y; \Theta)$, that if $T_x \gg \sigma_s$, then

$$\frac{J_{21}^2}{J_{11}J_{22}} \approx \frac{\sqrt{\pi}\sigma_s}{2T_x} \approx 0 \tag{7}$$

and hence, (3) reduces to (4). (A proof of this is easy but tedious; see [14] for details.) This result simply asserts that given enough observation area *across* the edge, uncertainty about I does not increase uncertainty about ℓ. In this case, there is enough information available to estimate both I and ℓ separately without incurring additional error.

III. The Canny Operator

Canny [8] presents an edge operator based on a linear filter $h_c(x, y)$, where the filter is chosen to optimize simultaneously output SNR and localization performance. For edges oriented parallel to the y axis, $h_c(x, y)$ is roughly the product $\phi'_{\sigma_c}(x) f_H(y)$ of the first derivative of a Gaussian function ϕ with scale σ_c and the Hanning window $f_H(y)$. For a Hanning window $f_H(y)$ of width T_y [16], we have

$$h_c(x, y) = \phi'_{\sigma_c}(x) f_H(y) = \left(\frac{-x}{\sqrt{2\pi}\sigma_c^3} e^{-\frac{x^2}{2\sigma_c^2}}\right)\left(\frac{1}{2} + \frac{1}{2}\cos(\frac{\pi}{T_y}y)\right)$$

for $|x| \leq T_x$ and $|y| \leq T_y$, and $h_c(x, y) = 0$ otherwise.

Canny's algorithm first filters an image $r(x, y)$ with several filters of the form $\phi'_{\sigma_c}(x) f_H(y)$, each with a different orientation, and subsequently locates the maximum by thresholding. We now analyze the localization performance of the Canny operator on the blurred and noise-corrupted step edge $r(x, y) = I\Phi(\frac{x-\ell}{\sigma_s}) + n(x, y)$. For simplicity, we do not consider the effect of orientation mismatch. If $h_c(x, y) = \phi'_{\sigma_c}(x) f_H(y)$ (which is properly oriented for our edge), we take the location estimate $\hat{\ell}_c$ to be where $\frac{\partial}{\partial x}(h_c(x, y) * r(x, y)) = 0$, or because h_c is smooth, we can use the condition $(\frac{\partial}{\partial x} h_c(x, y)) * r(x, y) = 0$. To analyze the error $\hat{\ell}_c - \ell$, we set $\ell = 0$ without loss of generality; then, the error is simply $\hat{\ell}_c$. As shown in the Appendix, high SNR approximate values for $E[\hat{\ell}_c]$ and $E[(\hat{\ell}_c)^2]$ are

$$E[\hat{\ell}_c] \approx 0.$$

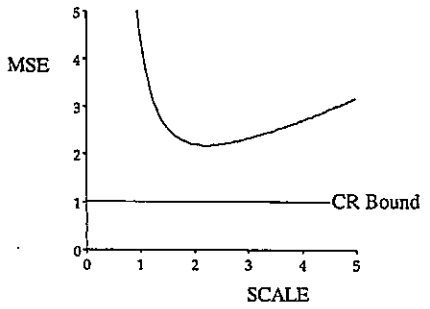

Fig. 2. MSE of the Canny estimate from (9) as the scale factor σ_c varies. The line indicates the Cramer-Rao lower bound (6) for the same values of N_0, I, T_y, and σ_s.

$$E[(\hat{\ell}_c)^2] \approx \frac{N_0^2 \int_{-T_y}^{T_y} f_H^2(y)dy \int_{-T_x}^{T_x} \left(o''_{\sigma_c}(x)\right)^2 dx}{\left[\int_{-T_y}^{T_y} f_H(y)dy\right]^2 \left[\int_{-T_x}^{T_x} o'''_{\sigma_c}(x) I\Phi(\frac{x}{\sigma_s})dx\right]^2}. \quad (8)$$

The variance $E[(\hat{\ell}_c)^2]$ can be simplified through straightforward integration [14]. We omit the intermediate steps, noting only that if for $T_x \gg \max(\sigma_c, \sigma_s)$, we use the approximation $\int_{-T_x}^{T_x} x^n \phi_\sigma(x)dx \approx E[x^n]$, then

$$E[(\hat{\ell}_c)^2] \approx \frac{9}{16} \frac{N_0^2 \sqrt{\pi}}{I^2 T_y} \frac{(\sigma_s^2 + \sigma_c^2)^3}{\sigma_c^5}. \quad (9)$$

When compared with the lower bound (6), this relation shows the effect on MSE of smoothing—as measured by σ_c—prior to edge estimation. Fig. 2 shows how $E[(\hat{\ell}_c)^2]$ varies as a function of σ_c. Differentiation shows that the minimum of $E[(\hat{\ell}_c)^2]$ occurs when $\sigma_c = \sqrt{5}\sigma_s$. For this value of σ_c, (9) yields

$$E[(\hat{\ell}_c)^2] \approx 2.2 \frac{N_0^2 \sqrt{\pi}\sigma_s}{I^2 T_y} \quad (10)$$

which is 2.2 times the CRLB in (6). Thus, for any value of σ_c, (9) is greater than the CRLB, and for the optimal value of $\sigma_c = \sqrt{5}\sigma_s$, (9) is 2.2 times (6). This is very good performance, but we show below that for high SNR, the ML estimator actually achieves the lower bound.

IV. Maximum Likelihood Estimates

The edge model $s(x, y; \Theta) = I\Phi(\frac{x-\ell}{\sigma_s})$ has two unknown parameters: $\theta_1 = I$ and $\theta_2 = \ell$. The maximum-likelihood (ML) estimates of both parameters satisfy the pair of equations [17]

$$\frac{1}{N_0^2} \iint_A \left[r(x,y) - s(x,y;\hat{\Theta})\right] \frac{\partial s(x,y;\Theta)}{\partial \theta_i}\Big|_{\hat{\Theta}} dxdy = 0. \quad i = 1, 2. \quad (11)$$

Substituting for $s(x, y; \Theta)$ yields the pair

$$-\iint_A \left[r(x,y) - \hat{I}\Phi(\frac{x-\hat{\ell}}{\sigma_s})\right] \hat{I}\phi_{\sigma_s}(x-\hat{\ell})dxdy = 0; \quad (12)$$

$$\iint_A \left[r(x,y) - \hat{I}\Phi(\frac{x-\hat{\ell}}{\sigma_s})\right] \Phi(\frac{x-\hat{\ell}}{\sigma_s})dxdy = 0. \quad (13)$$

Both equations can be solved for $\hat{I}$; equating the two solutions yields

$$\frac{\iint_A r(x,y)\phi_{\sigma_s}(x-\hat{\ell})dxdy}{\iint_A \Phi(\frac{x-\hat{\ell}}{\sigma_s})\phi_{\sigma_s}(x-\hat{\ell})dxdy} = \frac{\iint_A r(x,y)\Phi(\frac{x-\hat{\ell}}{\sigma_s})dxdy}{\iint_A \Phi^2(\frac{x-\hat{\ell}}{\sigma_s})dxdy}. \quad (14)$$

Let $n(\hat{\ell})$ be the ratio of denominators

$$n(\hat{\ell}) = \frac{\iint_A \Phi(\frac{x-\hat{\ell}}{\sigma_s})\phi_{\sigma_s}(x-\hat{\ell})dxdy}{\iint_A \Phi^2(\frac{x-\hat{\ell}}{\sigma_s})dxdy}$$

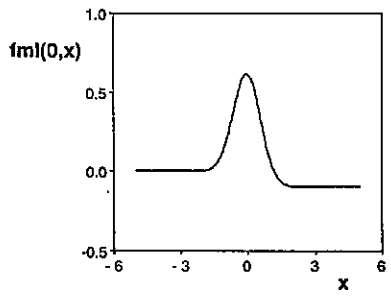

Fig. 3. Plot of maximum-likelihood filter f_{ml} along x axis when $\hat{\ell} = 0$ and $\sigma_s = 0.6$.

$$= \frac{\frac{1}{2}\left[\Phi^2(\frac{T_x-\hat{\ell}}{\sigma_s}) - \Phi^2(\frac{-T_x-\hat{\ell}}{\sigma_s})\right]}{\int_{-T_x}^{T_x} \Phi^2(\frac{x-\hat{\ell}}{\sigma_s})dx}. \quad (15)$$

Then, (14) can be rewritten as a single integral equation:

$$\iint_A r(x,y)\left[\phi_{\sigma_s}(x-\hat{\ell}) - n(\hat{\ell})\Phi(\frac{x-\hat{\ell}}{\sigma_s})\right]dxdy = 0. \quad (16)$$

Let $f_{ml}(\hat{\ell}, x)$ represent the term in [..]; it is a linear shift variant filter whose x cross section is shown in Fig. 3. Some intuition about the operation of this filter can be obtained by examining the approximate behavior of $n(\hat{\ell})$ when T_x is large and $\hat{\ell}$ is small:

$$n(\hat{\ell}) \approx \frac{\frac{1}{2}[1]}{\int_{-T_x}^{T_x} \Phi^2(\frac{x-\hat{\ell}}{\sigma_s})dx} \approx \frac{1}{2(T_x - \hat{\ell})}. \quad (17)$$

Under these conditions, we have $n(\hat{\ell}) \approx n(0)$, and consequently, f_{ml} varies very little with $\hat{\ell}$.

We now calculate the performance of the ML estimator. By replacing $r(x, y)$ with $I\Phi(\frac{x-\ell}{\sigma_s})$, it is easy to show that $\hat{\ell} = \ell$ satisfies (16), and thus, the ML estimator has zero systematic bias. To calculate bias and variance, we can set $\ell = 0$ without loss of generality and use the results in the Appendix, which show that for high SNR, $E[\hat{\ell}] \approx 0$ and

$$E[(\hat{\ell})^2] \approx \frac{N_0^2 \iint_A \left[\phi_{\sigma_s}(x) - n(0)\Phi(\frac{x}{\sigma_s})\right]^2 dxdy}{\left[\iint_A I\Phi(\frac{x}{\sigma_s})\left(-\frac{x}{\sigma_s^2}\phi_{\sigma_s}(x) - n'(0)\Phi(\frac{x}{\sigma_s}) + n(0)\phi_{\sigma_s}(x)\right)dxdy\right]^2}. \quad (18)$$

We use the approximation $n'(0) \approx \frac{1}{2T_x^2} \approx 0$ and $n(0) \approx \frac{1}{2T_x} \approx 0$ for $T_x \gg max(\sigma_s, 1.0)$; see (15) and (17). Then, (18) can be written as

$$E[(\hat{\ell})^2] \approx \frac{N_0^2\left[\int_{-T_x}^{T_x} \phi_{\sigma_s}^2(x)dx\right](2T_y)}{I^2[2T_y]^2\left[\int_{-T_x}^{T_x} \Phi(\frac{x}{\sigma_s})\phi'_{\sigma_s}(x)dx\right]^2}. \quad (19)$$

Integration by parts reveals that for $T_x \gg \sigma_s$, the integral in the denominator is approximately $-\frac{1}{2\sqrt{\pi}\sigma_s}$. Substituting this approximation, making a similar approximation in the numerator, and simplifying yields

$$E[(\hat{\ell})^2] \approx \frac{N_0^2 \sqrt{\pi}\sigma_s}{I^2 T_y} \quad (20)$$

which is the same as the CRLB specified in (6).

Our primary purpose here is to show that the CRLB can actually be achieved by a realizable estimator. We do not propose an algorithm for implementing f_{ml} because that would properly form the subject of another paper.

V. Conclusions

Our approach treats edge localization as a statistical parameter estimation problem and derives limits on attainable accuracy such as (6) or (3). As Section IV shows, for high SNR, the ML estimator attains these limits. Consequently, these expressions provide a simple and direct relationship between achievable MSE and the following factors: SNR, observation window size, and scale of smoothing filter.

We now consider some ramifications of our results. We chose to neglect the analysis of bias in our form of the CRLB. An alternative approach would be to formulate a lower bound on estimator error that makes no assumptions on bias, e.g. the Ziv-Zakai [19] or the rate-distortion [15] bounds. These bounds are generally tighter than the CRLB and provide more meaningful results for sharp intensity functions. The CRLB, however, is much simpler to evaluate and provides the easily interpreted result in (6), which is why it is used in this paper.

One might ask how our results, which were obtained in the continous domain, apply to real images, which are sampled and quantized. They apply in the sense that actual errors can only be worse than our error predictions: sampling and quantization errors necessarily degrade performance, and thus, the inequality on our CRLB is preserved. In a discretized image, a CRLB on subpixel edge localization can be derived using techniques similar to those used in this paper. It is doubtful, however, that simple analytical forms such as (6) could be obtained. We expect that numerical evaluation of the discrete domain bounds would behave similarly to the CRLB developed here but with higher error limits.

Finally, we note that of the topics left unstudied, perhaps the most interesting is the effect of orientation mismatch on directional operators such as Canny's [8]. If we include an unknown orientation parameter in our edge model, the Fisher matrix J in Section II becomes a 3×3 matrix. However, this small increase in the size of J increases considerably the calculations necessary for deriving analytical forms for the lower bounds. We leave these calculations for future work.

Appendix

We analyze the localization error $\hat{\ell} - \ell$ of a linear operator (see also [8]). Let $r(x, y) = I\Phi(\frac{x-\ell}{\sigma_s}) + n(x, y)$ be the received image, and assume that an estimate $\hat{\ell}$ of ℓ is formed by the condition

$$\left(\iint_A h(u, v, x, y) r(x, y) dx dy \right)_{u=\hat{\ell}} = 0. \tag{21}$$

Let $Hr(u, v)$ denote the integral above. After substituting for r, the condition can be written

$$Hs(\hat{\ell}, v) + Hn(\hat{\ell}, v) = 0, \tag{22}$$

where s is the edge $I\Phi(\frac{x-\ell}{\sigma_s})$, and n is the AWGN.

We are interested in the error $\hat{\ell} - \ell$ at any point v, say $v = 0$. We can set $\ell = 0$ without loss of generality, and the error is then simply $\hat{\ell}$. By expanding $Hs(\hat{\ell}, 0)$ in a Taylor series in u about $u = 0$, (22) becomes

$$Hs(0,0) + H_u s(0,0)\hat{\ell} + O(\hat{\ell}^2) + Hn(\hat{\ell}, 0) = 0 \tag{23}$$

where H_u denotes $\frac{\partial}{\partial u} H$. If the estimate has zero systematic bias, then $Hs(0,0) = 0$. Furthermore, if we take the error $\hat{\ell}$ to be small, which implicitly assumes high SNR, then we can neglect $O(\hat{\ell}^2)$. In addition, we can use the assumption that n is a uniform noise field to replace $Hn(\hat{\ell}, 0)$ by $Hn(0,0)$. On solving the resulting equation (23) for $\hat{\ell}$, we obtain

$$\hat{\ell} \approx -\frac{Hn(0,0)}{H_u s(0,0)} = -\frac{\iint_A h(0,0,x,y) n(x,y) dx dy}{\iint_A h_u(0,0,x,y) I\Phi(\frac{x}{\sigma_s}) dx dy}. \tag{24}$$

The mean and variance are now easily obtained:

$$E[\hat{\ell}] \approx 0; \qquad E[\hat{\ell}^2] \approx \frac{N_0^2 \iint_A (h(0,0,x,y))^2 dx dy}{\left[\iint_A h_u(0,0,x,y) I\Phi(\frac{x}{\sigma_s}) dx dy\right]^2}. \tag{25}$$

We see that for high SNR, the bias $E[\hat{\ell}] \approx 0$. To calculate the variance, we use $h(u, v, x, y) = \phi''_{\sigma_c}(u - x) f_H(v - y)$ for the Canny filter, and $h(u, v, x, y) = \phi_{\sigma_s}(x - u) - n(u)\Phi(\frac{x-u}{\sigma_s})$ for the ML estimator.

Acknowledgment

For their helpful comments, we thank the anonymous reviewers, especially the reviewer who suggested (17).

References

[1] E. P. Lyvers, O. R. Mitchell, M. L. Akey, and A. P. Reeves, "Subpixel measurements using a moment-based edge operator," *IEEE Trans. Patt. Anal. Machine Intell.*, vol. 11, no. 12, pp. 1293–1310, 1989.

[2] J. W. Burnett and T. S. Huang, "Image mensuration by maximum a posteriori probability estimation", *J. Opt. Soc. Amer.*, vol. 68, no. 2, 1978.

[3] W. E. L. Grimson, *From Images to Surfaces.* Cambridge, MA: MIT Press, 1981.

[4] A. J. Tabatabai and O. R. Mitchell, "Edge location to subpixel values in digital imagery," *IEEE Trans. Patt. Anal. Machine Intell.*, vol. PAMI-6, no. 2, pp. 188–201, 1984.

[5] A. Huertas and G. Medioni, "Detection of intensity changes with subpixel accuracy using lapacian-gaussian masks," *IEEE Trans. Patt. Anal. Machine Intell.*, vol. PAMI-8, no. 5, pp. 651–664, 1986.

[6] D. C. Marr and E. Hildreth, "Theory of edge detection", *Proc. Roy. Soc. London, B*, vol. B207, pp. 187–217, 1983.

[7] P. D. Hyde and L. S. Davis, "Subpixel edge estimation," *Patt. Recogn.*, vol. 16, no. 4, pp. 413–420, 1983.

[8] J. F. Canny, "A computational approach to edge detection", *IEEE Trans. Patt. Anal. Machine Intell.*, vol. PAMI-8, no. 6, pp. 679–698, 1986.

[9] M. Shah, A. Sood, and R. Jain, "Pulse and staircase edge models", *Comput. Vision Graphics Image Processing*, vol. 34, pp. 321–343, 1986.

[10] V. S. Nalwa and T. O. Binford, "On detecting edges," *IEEE Trans. Patt. Anal. Machine Intell.*, vol PAMI-8, no. 6, pp 699–714, 1986.

[11] V. Berzins "Accuracy of laplacian edge detectors," *Comput. Vision Graphics Image Processing*, vol. 27, pp. 195–210, 1984.

[12] D. I. Havelock, "Geometric precision in noise-free digital images," *IEEE Trans. Patt. Anal. Machine Intell.*, vol. PAMI-11, no. 10, pp. 1065–1076, 1989.

[13] R. A. Gonsalves, "Cramer-Rao bounds on mensuration errors," *Applied Opt.*, vol. 15, no. 5, 1976.

[14] R. Kakarala and A. O. Hero, "On achievable accuracy in edge localization," Tech. Memo., Commun. Signal Processing Lab., Dept. of EECS, Univ. of Michigan, Ann Arbor, Oct. 1990.

[15] A. Hero, "Lower bounds on estimator performance for energy-invariant parameters of multidimensional poisson processes," *IEEE Trans. Inform. Theory*, vol. 35, no. 4, pp. 843–859, 1989.

[16] S. M. Kay, *Modern Spectral Estimation: Theory and Application.* Englewood Cliffs, NJ: Prentice Hall, 1988.

[17] H. L. Van Trees, *Detection, Estimation, and Modulation Theory, Vol. I.* New York: Wiley, 1968.

[18] K. A. Winick, "Cramer-Rao lower bounds on the performance of charge-coupled-device optical position estimators," *J. Opt. Soc. Amer. A*, vol. 3, no. 11, pp. 1809–1815, 1986.

[19] J. Ziv and M. Zakai, "Some lower bounds on signal parameter estimation," *IEEE Trans. Inform. Theory*, vol. IT-15, no. 2, pp. 386–391, 1969.